FISCHER-TROPSCH SLURRY PHASE PROCESS VARIATIONS TO UNDERSTAND WAX FORMATIONS: QUARTERLY REPORT FOR PERIOD, APRIL 1, 1988-JUNE 30, 1988

MASSACHUSETTS INST. OF TECH., CAMBRIDGE.
DEPT. OF CHEMICAL ENGINEERING

1988

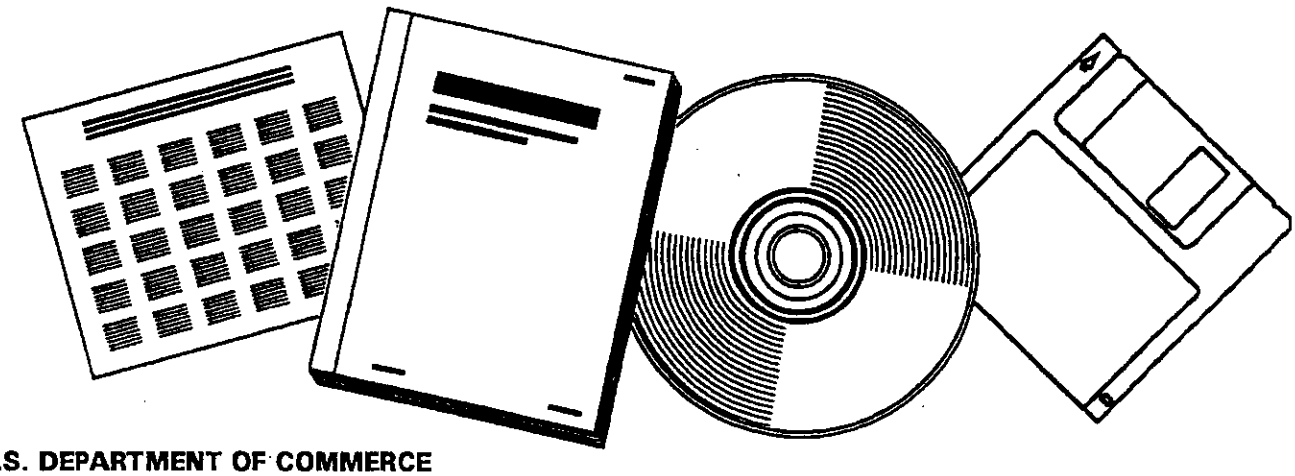

U.S. DEPARTMENT OF COMMERCE
National Technical Information Service

Fischer-Tropsch Slurry Phase Process Variations to Understand Wax Formations

Quarterly Report for Period April 1, 1988 to June 30, 1988

Report No.: DOE/PC80015-11

Contract No.: DE-AC22-85PC80015

DOE/PC/80015--11

DE88 012966

by

Timothy Donnelly and

Charles N. Satterfield

for

U.S. Department of Energy

Pittsburgh Energy Technology Center

P.O. Box 10940-MS 902-L

Pittsburgh, PA 15236

Attention: William E. McKinstry, Project Manager

Summary

A precipitated iron Ruhrchemie catalyst formerly used at the SASOL operations in South Africa and similar to that currently used was studied in a continuous-flow well-stirred slurry reactor at 232 C to 263°C, 2.16 to 2.98 MPa, H_2/CO feed ratios of 0.70 to 0.78 and syngas conversions of 15 to 65%. The carbon number distribution of the hydrocarbon products followed a Schulz-Flory distribution with two values of α. In general, α_1 was about 0.65 to 0.70 and α_2 for C_{25}-C_{35} products was 0.90. α_1 (calculated for C numbers of about 7 and below) decreases somewhat with increased temperature, while α_2 remained nearly constant. These distributions are compared to those of several other iron catalysts.

Selectivity to 1-alkenes increased with temperature. Secondary hydrogenation of 1-alkenes is shown to be a major pathway to n-alkanes. Activity for the water-gas shift is much less than that for other iron catalysts.

Introduction

Iron catalysts are used industrially in the two types of reactors presently in operation at the SASOL plants in South Africa, but details of catalyst composition and reactor operation have not been published and product compositions are generally reported only in terms of product groups such as wax, diesel fuel, gasoline, etc. The present study was performed with a sample of the precipitated iron catalyst manufactured by Ruhrchemie AG and formerly used in the low temperature, fixed-bed reactors at SASOL. Presently used catalysts in these reactors are believed to be fairly similar. The objective was to obtain detailed information on the product spectrum, including specific carbon number distributions, under well-defined and well-controlled reaction conditions. These results are then compared to well-documented results with other iron catalysts. The Ruhrchemie catalyst is heavily promoted with potassium and another objective was to compare the performance of this catalyst to that of a similar catalyst prepared in the same manner, but without potassium. That comparison will be made in a separate report.

The range studied here is that of general industrial applicability.

Experimental

1. Composition

The catalyst was supplied to us by Dr. Frohning of Ruhrchemie AG. Frohning (1977) describes the preparation method in detail, and a summary is given by Anderson (1984). The catalyst is precipitated from a hot solution of nitrates by the addition of Na_2CO_3. The precipitate is washed with distilled water to remove Na^+ ions, then slurried in water and impregnated with potassium water glass.

A sample of our catalyst was analyzed by atomic absorption spectroscopy by Galbraith Laboratories. Table 1 shows the results of duplicate analyses. Oxygen content, as determined by difference, is 34.4 wt%. This composition agrees with the range reported by Anderson.

2. Pretreatment

The catalyst was ground and sieved to 50 to 90 μm (170 to 270 ASTM mesh) and calcined in air at 130°C for 24 hours prior to reduction. The catalyst weight was reduced by about 2 wt% during calcination.

In the current experiments, the catalyst was reduced in a fixed bed unit under hydrogen at 0.21 MPa, according to instructions supplied by Ruhrchemie (Frohning, private comm.). 25.0 grams of catalyst were introduced to the reduction unit immediately after calcination. The temperature of the reduction tube was increased from ambient to 220°C over 3 hours while hydrogen passed upwards over the catalyst at 0.02 Nl/min/gcat.

The catalyst was held snug in the reduction unit by a glass wool plug. Reduction at 220°C was continued for 1 hour, then the reduction tube was weighed to determine the weight loss of the catalyst. The catalyst weight was reduced by 9.2 %, corresponding to about a 35 % removal of oxygen. This is a slightly milder reduction than that reported as typical by Anderson (1984).

A short set of experiments with another sample of this catalyst was performed by Matsumoto, but not reported. In that case the catalyst was reduced in situ in the slurry reactor. Activity was comparable to that for the current experiments. Light gas analyses for Matsumoto's set of experiments were similar to those obtained here.

3. Slurry Reactor Conditions

After reduction, the catalyst was charged to the one liter slurry reactor, in a nitrogen atmosphere, through a side port. Experiments were performed in a continuous-flow, well-stirred, one-liter slurry reactor. The system, analytical methods and method of operation are described in detail elsewhere (Huff and Satterfield, 1982, 1983; Matsumoto, 1987).

The reactor was first charged with 400 grams of recrystallized n-octacosane (melting point = 64.5°C, normal boiling point = 431.6°C). The n-octacosane was recrystallized in tetrahydrofuran (THF) to remove a bromine impurity introduced during synthesis from 1-bromo-tetradecane. After heating reactor contents to 190°C, the reduced catalyst was charged to the

reactor under nitrogen through a side port. Synthesis gas flow was started at 0.022 Nl/min/gcat from pre-mixed cylinders (Matheson). These were changed from time to time but at all times the gas feed had an H_2/CO ratio between 0.70 and 0.78. Synthesis gas conversion (H_2+CO) was varied over the range of 18 to 66%. The usage ratio is nearly the same as this feed ratio, so the exit H_2/CO ratio, which equals that throughout the reactor, was essentially the same as that in the inlet gas.

All the studies reported here were obtained on one batch of catalyst, with total time-on-stream of about 1200 hours. Studies were made at 232, 248, or 263°C, 2.16, 2.71, or 2.98 MPa, and flow rates of 0.010 to 0.035 Nl/min/gcat.

After a set of experimental conditions were established, at least 12 hours were allowed to elapse for steady state to be obtained and then samples were collected for typically 6 to 12 hours and an overall material balance calculated. The criteria for satisfactory results were several-fold. One was that an oxygen balance based on CO consumption versus CO_2 and H_2O formed should fall within 97.5% and 102%. (Oxygen present in the form of oxygenated organics is usually small.) Material balances were begun only after 88 hours on stream, to allow the catalyst to attain steady-state composition. At various sets of conditions, a series of 35 material balances was performed of which 27 were deemed to provide useful information. Conditions are shown on Table 2 and Table 5.

Periodic returns to "base-case" conditions of 248°C, 2.71

MPa, and 0.022 Nl/min/gcat indicated no appreciable deactivation of the catalyst during the run. Most of the results reported are based on product volatilized from the reactor, but slurry samples were also withdrawn periodically.

Results

1. Selectivity

Iron catalysts form primarily straight chain hydrocarbons, which are of value particularly for diesel fuel range products (about C_{10} to C_{20}). Methane is undesirable; $C_{20}+$ products (wax) are of low value as final components, but can be readily hydrocracked to diesel range products. Oxygenated organics are formed in modest amounts and generally must be removed. The focus of attention here was on carbon-number selectivity and how it is affected by process variables, such as reactor temperature, space velocity, H_2/CO feed ratio, and hydrogen pressure. Some information on component selectivities is also provided.

The complete data for these experiments are given in Appendix A, in the form of results files for completed material balances. Table 2 is a summary of the important selectivity information.

1.1 Carbon Number Distribution

The carbon number distribution of the hydrocarbon products follows a Schulz-Flory model with two chain growth parameters, α_1 and α_2 and a "break-point" near C_7. A non-linear least squares regression of semi-logarithmic data, as recommended by Donnelly, Yates, and Satterfield (in press), was used to calculate values

for α_1 and α_2 for 20 of the material balances for which this could be done. In each case, C_1 to C_{16} data were used as input and C_3 to C_{16} data were regressed using a FORTRAN routine to determine the best fit. Figure 1 shows an example of the total organics product distribution (paraffins plus olefins plus oxygenates) fitted by the non-linear regression. As an indication of the repeatability of our experiments, figure 2 shows, on one Schulz-Flory diagram, the results of 4 material balances performed at 263°C and 2.7 to 3.0 MPa.

Figure 3 is a Schulz-Flory diagram of a wax sample withdrawn from the reactor after 150 hours-on-stream. Analysis was by temperature-programmed vapor-phase chromatography (see, e.g., Stenger, Johnson and Satterfield, 1984).). Below about C_{20} most of the products are volatilized out of the reactor. Beyond the maximum on the graph, the products remain in the pot liquid increasingly with increased carbon number. Oxygenates are negligible in the wax and paraffins plus olefins are summed for each C number. The value of α_2 was determined by linear regression of the C_{25}-C_{35} range, excluding C_{32} which includes an impurity. For this sample, α_2 is 0.88 and for similar samples drawn at 600 and 1200 hours-on-stream and α_2 was found to be 0.91 and 0.89, respectively. Values of α determined in this fashion represent the cumulative effects of all process changes.

To allow comparison with data reported by Huff (1982) and Matsumoto (1987), C_3 to C_7 mole fractions were also regressed linearly to determine a value for α_1. The values calculated by

the linear and non-linear regression techniques agreed within about 5 %, except at high values of α_1 ($\alpha_{1,lin-reg} > 0.75$). The reasons for the differences between linearly and non-linearly regressed values are discussed in detail elsewhere (Donnelly, Yates, and Satterfield, in press). Effects of operating conditions on α_1 are reported for the linear-regressed values, while effects on α_2 are reported for the non-linear regressed values.

1.1.1 Effect of Temperature

Figure 4 shows that α_1 decreased from about 0.75 at 232°C to about 0.66 at 263°C. On the same figure, α_2 is shown to be nearly constant with temperature, with a value between 0.89 and 0.92. Matsumoto likewise reported values of α_2 of about 0.89-0.93 over this temperature range, on a reduced fused magnetite catalyst.

Dictor and Bell (1986) have reported that α_1 decreases with increasing temperature. Their data, collected using precipitated iron catalysts, with and without potassium promoter, are in good agreement with ours. Dry (1983) also reports a shift to lighter products at high temperature for the SASOL reactors.

1.1.2 Effect of Space Velocity

Figure 5 shows that both chain growth probabilities are relatively constant with space velocity. This indicates that synthesis gas conversion, in the range 15 to 60%, is not an important variable in determining carbon number distribution. This is reasonable for the studies here in which feed ratio and

usage ratio are nearly the same.

1.1.3 Component Schulz-Flory Diagrams

Figure 6 is a Schulz-Flory diagram for overhead products in material balance 16, including the component distributions for n-alkanes, 1-alkenes, and oxygenates. Both 1-alkenes and n-alkanes display a double-α, as does the overall product distribution. Only oxygenates can be characterized by a single α. Alkanes dominate the product distribution at high carbon numbers. This diagram is representative of data obtained in general. The values of the component and total chain growth probabilities are given in Table 3 for two material balances.

Clear evidence here of a double-α for 1-alkenes contrasts with the conclusion reached by Egiebor, Cooper, and Wojciechowski (1985), who reported a single-α for all product classes except n-alkanes. Their interpretation was based on a rather complicated kinetic model which assumes different termination steps for alkanes and alkenes, the rates of which are dependent on carbon number. However there is now substantial evidence that olefins are hydrogenated to paraffins by a secondary reaction and so the olefins product distribution is essentially a happenstance determined by operating conditions.

The increasing shift to paraffins at high carbon numbers is readily understood as secondary hydrogenation which becomes increasingly important for heavier alkenes, which have increased residence time in the reactor. The importance of secondary hydrogenation is demonstrated below in 1.2.1.3.

1.1.4 Comparison With Other Catalysts

Table 4 is a comparison of the selectivities of several iron catalysts to product cuts of interest. The Mobil catalysts were precipitated iron catalysts of unspecified composition but prepared in two different ways to alter the extent of wax formation. They were studied extensively on a pilot plant scale and considerable information on their performance is available. The Mobil "high wax" catalyst and the SASOL fixed bed catalyst show the highest selectivities to diesel fuel and wax. The selectivity of the Ruhrchemie catalyst studied here is comparable to that of an alkalized catalyst prepared and tested by Pittsburgh Energy Technology Center (PETC), and similar to the selectivity of a PETC catalyst to which potassium tert-butoxide was added in situ in our reactor. The United Catalysts C-73 fused magnetite catalyst shows the greatest selectivity to light products. An unalkalized PETC precipitated iron catalyst shows selectivity comparable to the C-73 catalysts.

1.2 Component Selectivities

1.2.1 1-alkene/n-alkane Ratio

C_4 products are used as examples for this study, since they exist only in the gas phase at ambient conditions, so no problems are encountered with product splitting between gas and liquid phases.

For the material balances here, the ratio of 1-butene/n-butane was between 3.1 and 5.7. At higher carbon numbers, the 1-alkene/n-alkane ratio decreased, most probably caused by

secondary hydrogenation.

1.2.1.1 Temperature Dependence

Figure 7 shows that the 1-butene/n-butane ratio increases almost linearly with temperature over the range 232 to 263°C, from about 3.1 to 4.5. Anderson (1956) and Huff (1982) have found similar results on precipitated and fused iron catalysts, respectively.

1.2.1.2 Space Velocity Dependence

Figure 8 indicates that the 1-butene/n-butane ratio is independent of space velocity. Huff (1982) and Weitkamp, et. al. (1953) have also reported that space velocity does not affect alkene/alkane ratio.

1.2.1.3 Kinetic Modelling of 1-Alkene Hydrogenation

It is reasonable to suppose that a significant fraction of the paraffins produced in the Fischer-Tropsch Synthesis are secondary products, resulting from olefin hydrogenation. It is of interest to know the dependence of olefin hydrogenation on the composition of the gases in the reactor.

The hydrogenation of an adsorbed olefin, say 1-butene, can be written as:

$$C_4H_8 + H_2 \longrightarrow C_4H_{10} \qquad (1)$$

We ignore hydrogenation of 2-alkenes, which Sudheimer and Gaube (1985) have shown to proceed very slowly, relative to 1 -alkene hydrogenation. The rate expression for 1-butene hydrogenation is:

$$R_{butane} = k\, P_{H_2}\, \theta_{1\text{-butene}} \qquad (2)$$

It is possible that competitive adsorption by carbon monoxide could inhibit 1-butene hydrogenation. Assuming complete coverage, $\theta_{1\text{-butene}}$ can be written:

$$\theta_{1\text{-butene}} = \frac{K_{1\text{-butene}}\, P_{1\text{-butene}}}{K_{CO}\, P_{CO}} \qquad (3)$$

Substituting equation (3) into equation (2) and rearranging:

$$\frac{P_{H_2}}{R_{butane}} = \frac{K_{CO}}{k\, K_{1\text{-butene}}} \times \frac{P_{CO}}{P_{1\text{-butene}}} \qquad (4)$$

Equation (4) implies a linear relationship, with the intercept depending only on the relative adsorptivities and a rate constant.

Figure 9 is a plot of equation (4) using all usable data (Table 5). Three symbols are used to represent different space velocities, and it can be seen that with the assumed model, the hydrogenation rate decreases at high conversion. This suggests that competitive adsorption by 1-alkene products could inhibit hydrogenation; however, attempts to fit the current data with a model allowing for alkene inhibition do not explain the conversion dependence. Data from an unalkalized precipitated iron PETC catalyst are fit well by a model with terms for inhibition by 1-alkenes and CO, as shown in a separate report.

We also attempted to model the hydrogenation reaction by including a term allowing for inhibition by water, but this did not improve the fit either. Higher order inhibition models can not be justified physically. No explanation is offered at this time for the conversion dependence of hydrogenation rate.

Examination of Figure 9 indicates that all n-butane production can be attributed to hydrogenation. Hanlon and Satterfield (1988) have reported that the principal reactions of 1-alkenes added to a slurry reactor are hydrogenation and some isomerization. Anderson (1956) has also reported that olefins are readily hydrogenated to paraffins. Schulz, Rao, and Elstner (1970) have also shown through isotopic labelling experiments that paraffins are produced predominantly by the hydrogenation of 1-alkenes. The current data agree with all of these studies.

An important result of the observation that paraffins are produced predominantly as secondary products is that α_1 and α_2 for n-alkanes and 1-alkenes reflect the influence of both chain growth and hydrogenation, and that the much higher value of α_2 for n-alkanes may be due largely to secondary hydrogenation.

1.2.2 2-alkene/1-alkene Ratio

Essentially no 2-alkenes were observed.

1.2.3 Methane Production

Methane production accounted for about 20 to 28 mole% of the hydrocarbon plus oxygenated products of the Fischer-Tropsch synthesis. This corresponds to about 3 to 6 wt%.

Dry (1976) has noted that methane selectivity is closely related to other selectivities, so the changes in CH_4 observed with changes in operating parameters may be correlated to changes in overall product distribution.

1.2.3.1 Temperature Dependence

It is difficult to decouple the dependence of methane

production on temperature from the overall product shift to lower molecular weight at higher temperatures. Figure 10 shows the mole fraction of products as methane versus temperature and indicates a general shift to higher methane fraction at higher temperature.

1.2.3.2 Space Velocity

Figure 11 shows that the mole fraction of products as methane does not depend on space velocity, at a fixed temperature.

1.2.3.3 Hydrogen Partial Pressure Dependence

It is worthwhile to consider the production of methane as a hydrogenation, as butane production was considered above. Figure 12 shows the dependence of methane production rate on hydrogen partial pressure at 263°C. A general increase is observed, although the effect is weaker at lower temperatures.

1.2.4 Oxygenate Production

Oxygenates generally constituted 4 to 9 wt% of the products. Normal alcohols were the predominant oxygenated species, with small amounts of aldehydes and ketones, and only traces of light carboxylic acids. Ethanol generally accounted for approximately half of the weight of oxygenates produced.

1.2.4.1 Temperature Dependence

Figure 13 is a plot of the weight percent of oxygenates in the product as a function of temperature. The data indicate very little relationship between temperature and oxygenate production.

1.2.4.2 Space Velocity Dependence

Figure 14 indicates that the weight percent of oxygenates is also independent of space velocity over the range studied.

1.2.4.3 Time-on-Stream Dependence

While the selectivities to methane and to alkenes can be attributed to operating parameters, no such correlation was observed for oxygenates. However, the weight percent of oxygenates roughly doubled over the course of 1200 hours-on-stream, as shown on Figure 15 for various material balance numbers done at 248°C. This could well be caused by a change in oxidation state of the catalyst. Satterfield, et. al. (1986) have reported such a phase change, based on Mössbauer spectroscopy.

2. Activity and Kinetics

The experiments here were performed with the goal of obtaining selectivity information, rather than detailed kinetic models, so the information reported on activity and kinetics is of only a general nature. Appendix A includes some activity information; however, the more detailed information used in this report is summarized in Table 6.

2.1 Intrinsic Fischer-Tropsch Kinetics

The intrinsic kinetics of the Fischer-Tropsch synthesis on iron catalysts have been studied and reviewed by Anderson (1956), Vannice (1976), Dry (1981), and Frohning, et. al. (1982), among others. Huff and Satterfield (1984b) have presented a detailed review and proposed a kinetic model, which they show to fit data for an alkalized, fused iron catalyst over a variety of conditions.

Figure 16 shows the rate of conversion of synthesis gas as a function of hydrogen partial pressure. A simple first-order dependence with a zero-intercept fits the data reasonably well and is used to compare catalyst activities. Twenty material balances from the middle of the run were used for kinetic modelling. No deactivation of the catalyst was observed during the first 25 material balances, as can be seen from the data in Table 6. Material balances 25 to 31 were performed with the reactor head heated externally and were not considered for kinetic modelling, as the observed rates were about 20% greater.

More detailed kinetic models based on Langmuir-Hinshelwood formulations, such as Huff and Satterfield's equation (25) did not show improved fit to the current data:

$$P_{H_2}/(-R_{H_2+CO}) = (1/ab')\ P_{H_2O}/(P_{CO}P_{H_2}) + 1/a \qquad (4)$$

This may be due to the unusually high partial pressures of water (up to 0.24 MPa), caused by the low activity of this catalyst for the water-gas shift, or to the relatively small range of H_2/CO ratios in situ (0.59 to 0.66). Similarly, an attempt to use a "semi-fundamental" power-law rate expression, as presented by Anderson, Karn, and Shultz (1964) did not improve the correlation of data.

Figure 17 shows the relative usage of hydrogen as a function of CO + H_2 conversion, based on all useful data obtained. The behavior shown in Figure 17 agrees closely with a plot given by Anderson, Karn, and Shultz (1964) for a nitrided fused iron catalyst. They conclude that the rate of water-gas shift was nearly the same as the rate of primary Fischer-Tropsch synthesis, but the ratio of the two can vary substantially with the nature of the iron catalyst.

The simple first-order hydrogen dependence is able to describe catalyst activity well over the range of reactor conditions studied here.

2.2 Catalyst Activity

The intrinsic activity of this catalyst for the Fischer-Tropsch synthesis, defined as mmol($CO+H_2$) converted per minute per gram of unreduced catalyst, is low relative to several other